第 28 卷第 6 期 热能动力工程 Vol. 28, No. 6
2013 年 11 月 JOURNAL OF ENGINEERING FOR THERMAL ENERGY AND POWER Nov., 2013

文章编号: 1001 - 2060(2013) 06 - 0644 - 06

基于太阳能集热技术的火电厂 CO_2 捕集系统性能研究

陈海平[1], 于鑫玮[2], 鲁光武[2]
(1. 华北电力大学 能源动力与机械工程学院, 国家火力发电工程技术研究中心, 北京 102206;
2. 华北电力大学 能源动力与机械工程学院, 河北 保定 071003)

摘 要: 针对燃煤电厂 CO_2 捕集技术的高能耗问题, 阐述了新型抛物面槽式太阳能集热系统、胺基 CO_2 捕集系统与燃煤机组热力系统的耦合机理, 基于等效焓降法理论, 针对 300 MW 燃煤机组计算分析了各个集成方案的热经济性, 得出了太阳能供能条件下, 拥有胺基 CO_2 捕集系统的机组热经济性变化规律以及扩容蒸发器中疏水与再沸器饱和水的最佳回水位置及其规律。结果表明, 当预热段进口水引自凝结水泵出口时, 机组循环热效率随碳捕捉率的增加而提高, 当预热段进口水引自给水泵出口时, 与之相反; 扩容蒸发器及再沸器饱和水的最佳回水位置为机组主凝结水管路 6 号加热器出口, 预热段由凝结水泵出口引入水份额为 40% 时, 节省标煤耗率 0.31 g/(kW·h), 碳捕捉率达 43.86%。

关 键 词: CO_2 捕集; 太阳能集热系统; 等效焓降法; 热经济性

中图分类号: TM615 **文献标识码**: A

引 言

基于单乙醇胺(MEA) 燃烧 CO_2 捕集是目前最成熟的 CO_2 捕集技术[1~3], 已在华能北京热电厂成功示范运行[4], 该技术使用汽轮机某级低压抽汽减压降温后作为溶剂再生热源, 这将使机组效率降低 6 ~15 个百分点。鉴于此, 本研究遵循能量"品位对口、梯级利用"的原则[5], 将新型抛物槽式太阳能集热系统、胺基 CO_2 捕集系统与燃煤机组热力系统进行集成, 合理利用能量密度低的太阳能提供品位低的热能作为胺基 CO_2 捕集系统的溶剂再生热源, 以实现燃煤机组节能减排的目的。以国产某 300 MW 火电机组为为例进行分析, 以期为火电厂燃烧后胺基 CO_2 的高效捕集技术提供科学依据。

1 新型抛物面槽式太阳能集热系统

1.1 太阳能集热系统优化设计

太阳能集热系统过热段出口蒸汽用于火电厂燃烧后胺基 CO_2 捕集再沸器溶剂的再生。因此太阳能集热系统采用定出口温度运行方式, 使得集热系统过热段出口蒸汽参数达到溶剂再生所需要的蒸汽参数的要求。

由于传统太阳能集热系统预热段会产生汽液两相流状态, 传热效果恶化[2], 因此采用扩容蒸发器代替传统的汽水分离器, 通过扩容蒸发器的合理布置以及管路的局部调整, 扩容蒸发器中产生的温度较高的疏水不再是经再循环泵回到预热段入口, 而是经过疏水泵输送到机组给水或凝结水系统, 控制预热段出口处的工质水温度小于或等于相应压力下的饱和水温度, 使得该集热系统预热段工质始终处于单相流状态, 然后再经过扩容蒸发器(如图 1 所示) 进行扩容蒸发, 产生相应压力的蒸汽经过过热段进行加热, 最后达到再沸器溶剂再生所需要的蒸汽参数的要求被送到再生系统。新型抛物槽式太阳能集热系统的设计如图 2 所示。

图 1 扩容蒸发器实物图
Fig. 1 Chart showing the real object of the flash evaporator

1.2 太阳能集热系统运行参数

扩容蒸发器汽水比是扩容蒸发器一项重要参数, 由扩容蒸发器进口工质压力及自身压力决定, 经模拟分析可得扩容蒸发器汽水比随扩容蒸发器进口

收稿日期: 2013 - 03 - 22; 修订日期: 2013 - 05 - 31
作者简介: 陈海平(1963 -), 男, 内蒙古托克托人, 华北电力大学教授, 博士.

工质压力以及扩容蒸发器压力的变化关系曲线，如图3所示。

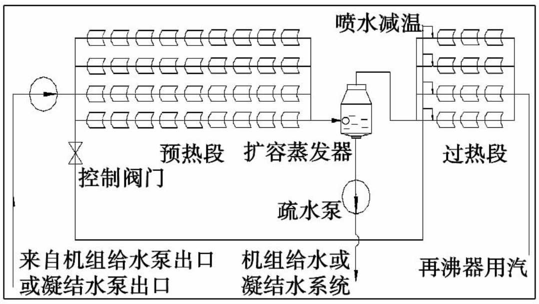

图2　新型抛物面槽式太阳能集热系统

Fig. 2 New type parabolic trough solar heat collection system

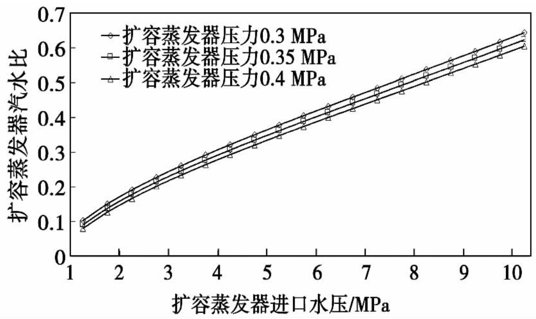

图3　汽水比与扩容蒸发器进口水压力以及扩容蒸发器压力的关系

Fig. 3 Relationship among the steam/water ratio, water pressure at the inlet of the flash evaporator and pressure in the flash evaporator

胺基CO_2捕集溶剂再生所需的热负荷较高，并且对换热工质参数要求苛刻，因此扩容蒸发器汽水比将直接影响溶剂的再生能力，进而影响CO_2捕捉效率，根据参考文献[4,7]，用于溶剂再生的换热工质水蒸气温度为144 ℃，压力为0.3～0.4 MPa。

当扩容蒸发器压力一定时，扩容蒸发器汽水比随扩容蒸发器进口水压的提高而增大，太阳能集热器吸热管的耐压能力有限，一般不超过10 MPa[8]，为获得较高的碳捕捉率，应尽可能提高扩容蒸发器进口水压；当扩容蒸发器进口水压力一定时，扩容蒸发器汽水比随其自身压力的提高而减小，若扩容蒸发器压力较小，虽然碳捕捉率有所提高，但过热段出口蒸汽与MEA富液换热并且其溶剂MEA得到再生后成为回水与扩容蒸发器中疏水汇合后一同返回机组热力系统，两股水流的参数较低将会影响机组热经济性。

2　燃烧后胺基CO_2捕集工艺

燃烧后胺基CO_2捕集系统安装在燃煤电厂锅炉烟气脱硫系统之后。从脱硫系统出来的烟气经除水、降温至40 ℃左右后经风机进入吸收塔，与MEA贫液逆流混合，净化后烟气从吸收塔顶引出。吸收CO_2后的富液在富液泵作用下从吸收塔储液槽，通过贫富液换热器，被高温的贫液加热后从再生塔上部进入再生系统。再生系统中再沸器为管壳式换热器，壳程内为太阳能集热系统产生的微过热蒸汽，管程内为胺溶液。胺溶液经过再沸器，温度被加热到110 ℃左右，发生可逆分解反应。解析出的CO_2连同水蒸气进入闪蒸罐分离可得到纯度较高的CO_2产品，可用于食品加工、制冷等。由再生塔底的贫液在贫液泵作用下经贫富液换热器与补充的胺溶液混合后经贫液冷却器冷却进入吸收塔。胺基CO_2捕集系统工艺流程如图4所示。

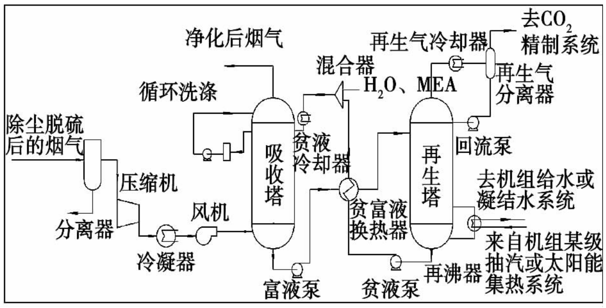

图4　胺基CO_2捕集系统工艺流程图

Fig. 4 Chart showing the flow path of the amidogen-based CO_2 capture system

3　集成系统工艺流程

图5给出了基于新型抛物槽式太阳能集热技术的胺基CO_2捕集系统与300 MW燃煤机组热力系统的集成系统工艺示意图。预热段进口工质引自机组凝结水泵或给水泵出口水，经太阳能集热系统后被加热至压力0.4 MPa、温度144 ℃的微过热蒸汽，以此作为CO_2捕集溶液再生热源（汽轮机第五段抽汽作为辅助热源），利用其汽化潜热来提供再沸器溶剂再生所需的热负荷，再沸器回水与扩容蒸发器中疏水一同返回机组给水或者凝结水系统。

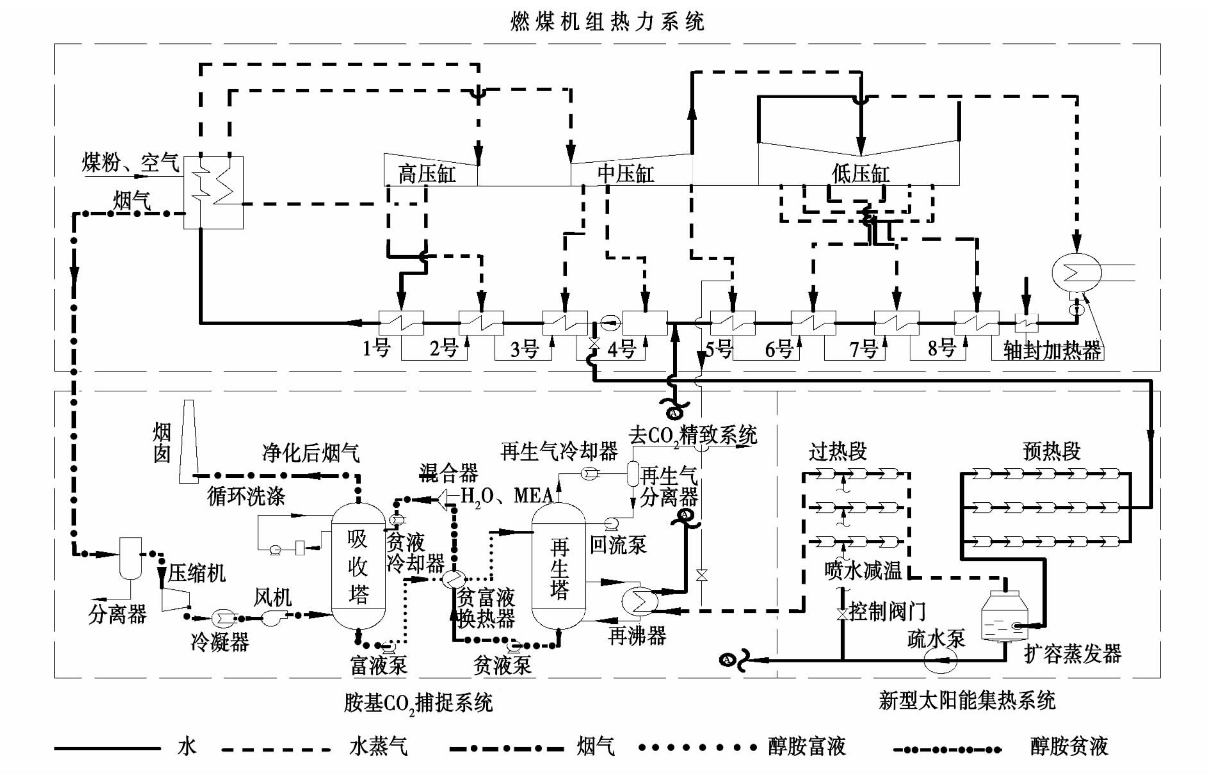

图 5　集成系统工艺流程图

Fig. 5 Chart showing the flow path of the integrated system

4　集成系统性能分析

依据表 1 数据，机组额定工况下新蒸汽等效焓降[9]、循环吸热量、汽轮机组绝对内效率分别为：

$$H_0 = h_0 + \sigma - h_c - \sum_{i=1}^{8} \tau_i \eta_i^0 - \sum \Pi = 1\,222.803 \text{ kJ/kg} \quad (1)$$

$$Q_0 = h_0 + \alpha_{zr}\sigma - h_{gs} + \tau_p = 2641.47 \text{kJ/kg} \quad (2)$$

$$\eta_0 = H_0 / Q_0 = 0.46293 \quad (3)$$

式中：h_0—主蒸汽焓；σ—再热吸热量；h_c—排汽焓；τ_i—i 号加热器的给水焓升；η_i^0—i 段抽汽的抽汽效率；$\sum \Pi$—各种附加成分做功损失之和；α_{zr}—再热蒸汽份额；h_{gs}—主给水焓；τ_p—给水泵功；H_0—新蒸汽等效焓降；Q_0—机组循环吸热量。

表 1　机组回热加热系统汽水参数

Tab. 1 Parameters of the steam and water parameters of the regenerative heating systemof the unit

汽水参数	抽汽或加热器序号							
	1	2	3	4	5	6	7	8
抽汽焓 h_i/kJ · kg^{-1}	3140.5	3021.6	3327.4	3157.5	3009.5	2878.7	2751.1	2622.6
给水焓 h_{wi}/kJ · kg^{-1}	1200.6	1045.7	853.2	746.8	611.2	519.0	434.0	346.0
疏水焓 h_{di}/kJ · kg^{-1}	1070.4	870.2	760.8	—	541.2	455.6	367.2	179.5
抽汽放热量 q_i/kJ · kg^{-1}	2070.1	2151.4	2566.6	2546.3	2468.3	2423.1	2383.9	2463.7
给水焓升 τ_i /kJ · kg^{-1}	154.9	192.5	106.4	135.6	92.2	85.0	88.0	187.1
疏水放热量 γ_i /kJ · kg^{-1}	—	200.2	109.4	149.6	—	85.6	88.4	208.3
抽汽效率 η_i^0	0.5130	0.4833	0.3378	0.2909	0.2484	0.2063	0.1622	0.1144

太阳能集热系统预热段进口工质引自机组给水泵或凝结水泵出口，给水泵或者凝结水泵出口水出系统带工质热量出系统新蒸汽等效焓降变化量计算式为：

$$\Delta H_1 = \begin{cases} -\alpha_{in}\sum_{i=4}^{8}\tau_i\eta_i^0 & \text{给水泵出口水} \\ -\alpha_{in}(h_{wc}-h_{bs}) & \text{凝结水泵出口水} \end{cases} \tag{4}$$

式中：α_{in}—进入太阳能集热系统水的份额；h_{wc}—凝结水泵出口水焓；h_{bs}—凝汽器补水焓。

扩容蒸发器中疏水以及再沸器饱和水从机组 i 号加热器给水或凝结水管路以及疏水管路出口汇入系统新蒸汽等效焓降增加计算式为：

$$\Delta H_2 = \begin{cases} (\alpha_{fyr}+\alpha_{zf})\left[(h_{fyr}-h_{wi})\eta_{i-1}^0+\sum_{r=i}^{8}\tau_r\eta_r^0\right] \\ \text{汇入主给水或凝结水管路} \\ (\alpha_{fyr}+\alpha_{zf})\left[(h_{fyr}-h_{di})\eta_{i+1}^0+\sum_{r=i+1}^{m}\gamma_r\eta_r^0+\sum_{r=m+1}^{8}\tau_r\eta_r^0\right] \\ \text{汇入疏水管路} \end{cases} \tag{5}$$

式中：α_{fyr}—扩容蒸发器中疏水份额；α_{zf}—再沸器饱和水份额；h_{wi}—i 号加热器出口给水焓；h_{di}—i 号加热器出口疏水焓；h_{fyr}—扩容蒸发器中疏水与再沸器回水平均焓值；η_r^o—r 段抽汽的抽汽效率；；τ_r—r 号加热器的给水焓升；γ_r—r 号加热器的疏水放热量。

因此，太阳能集热系统以及胺基 CO_2 捕集系统的引入引起机组总的新蒸汽等效焓降变化量为：

$$\Delta H = \Delta H_1 + \Delta H_2 \tag{6}$$

式中：ΔH_1—给水泵或者凝结水泵出口水携带热量引起新蒸汽等效焓降变化量；ΔH_2—扩容蒸发器中疏水以及再沸器饱和水从机组 i 号加热器给水或凝结水管路以及疏水管路出口汇入引起新蒸汽等效焓降增加量。

从而可计算出预热段进口水从凝结水泵或给水泵出口引入对太阳能集热系统应不同扩容蒸发器及再沸器回水汇入点时的机组热经济性指标如表2和表3所示。

表2　预热段进口水从凝结水泵出口引入时各个集成方案系统热经济性指标

Tab.2 Thermo－economic indicators of the system in various integrated versions when water at the inlet of the preheating section is introduced from the outlet of the condensatge pump

集成方案		新蒸汽等效焓降变化量 ΔH /kJ·kg^{-1}	汽轮机绝对内效率 /%	汽轮机绝对内效率相对变化值/%	全厂循环热效率/%	全厂热耗率 /kJ(kW·h)$^{-1}$	标煤耗率 /g(kW·h)$^{-1}$	碳捕捉率/%	太阳能集热器场面积/m^2
扩容蒸发器及再沸器回水汇入点	预热段进口水流量份额/%								
5号低加给水出口	10	0.2876	46.303	0.0235	40.231	8948.30	305.733	10.97	49631.3
	20	0.5753	46.314	0.0470	40.241	8946.19	305.662	21.94	99262.7
	30	0.8629	46.325	0.0705	40.250	8944.09	305.590	32.90	148894.0
	40	1.1505	46.336	0.0940	0.4026	8941.99	305.518	43.86	198525.3
6号低加给水出口	10	0.3154	46.304	0.0258	40.232	8948.09	305.726	10.97	49631.3
	20	0.6308	46.316	0.0516	40.242	8945.79	305.648	21.94	99262.7
	30	0.9461	46.328	0.0773	40.253	8943.48	305.569	32.90	148894.0
	40	1.2615	46.340	0.1031	40.263	8941.18	305.490	43.86	198525.3
5号低加疏水出口	10	−0.2419	46.283	−0.0198	40.214	8952.17	305.866	10.97	49631.3
	20	−0.4840	46.274	−0.0396	40.206	8953.94	305.926	21.94	99262.7
	30	−0.7256	46.265	−0.0594	40.198	8955.72	305.987	32.90	148894.0
	40	−0.9675	46.256	−0.0792	40.190	8957.49	306.047	43.86	198525.3
7号低加给水出口	10	−0.0453	46.291	−0.00004	40.220	8950.73	305.817	10.97	49631.3
	20	−0.0906	46.290	−0.00007	40.219	8951.06	305.828	21.94	99262.7
	30	−0.1359	46.287	−0.00011	40.217	8951.40	305.839	32.90	148894.0
	40	−0.1812	46.286	−0.00015	40.216	8951.73	305.851	43.86	198525.3

表 3 预热段进口水从给水泵出口引入时各个集成方案系统热经济性指标

Tab. 3 Thermo-economic indicators of the system in various integrated versions when water at the inlet of the preheating section is introduced from the outlet of the feedwater pump

集成方案		新蒸汽等效焓降变化量 ΔH /kJ·kg^{-1}	汽轮机绝对内效率 /%	汽轮机绝对内效率相对变化值/%	全厂循环热效率/%	全厂热耗率 /kJ·(kW·h)$^{-1}$	标煤耗率 /g·(kW·h)$^{-1}$	碳捕捉率/%	太阳能集热器场面积/m^2
扩容蒸发器及再沸器回水汇入点	预热段进口水流量份额/%								
5 号低加给水出口	10	-4.1346	46.136	-0.3393	40.086	8980.77	306.843	10.97	26194.5
	20	-8.2691	45.979	-0.6808	39.950	9011.34	307.887	21.94	52389.0
	30	-12.4037	45.823	-1.0247	39.814	9042.12	308.939	32.90	78583.5
	40	-16.5382	45.666	-1.3710	39.678	9073.11	309.998	43.86	104778.0
6 号低加给水出口	10	-4.1068	46.137	-0.3370	40.087	8980.56	306.836	10.97	26194.5
	20	-8.2136	45.982	-0.6762	39.951	9010.93	307.873	21.94	52389.0
	30	-12.3204	45.826	-1.0178	39.816	9041.50	308.918	32.90	78583.5
	40	-16.4272	45.671	-1.3617	39.681	9072.28	309.970	43.86	104778.0
5 号低加疏水出口	10	-4.6641	46.116	-0.38295	40.068	8984.67	306.976	10.97	26194.5
	20	-9.3281	45.939	-0.7687	39.915	9019.21	308.156	21.94	52389.0
	30	-13.9922	45.763	-1.1575	39.761	9054.00	309.345	32.90	78583.5
	40	-18.6563	45.586	-1.5493	39.608	9089.07	310.543	43.86	104778.0
7 号低加给水出口	10	-4.4675	46.123	-0.3667	40.075	8983.22	306.927	10.97	26194.5
	20	-8.9350	45.954	-0.7360	39.928	9016.28	308.056	21.94	52389.0
	30	-13.4024	45.785	-1.1082	39.781	9049.59	309.194	32.90	78583.5
	40	-17.8700	45.616	-1.4831	39.634	9083.14	310.341	43.86	104778.0

由表 2 及表 3 数据可以得出，扩容蒸发器中疏水及再沸器回水汇入点为主凝结水管路 6 号低加给水出口时对机组热经济性最有利；太阳能集热系统预热段工质选取不同引水点时使得机组热经济性随碳捕捉率的增加有很明显的变化规律，当预热段进口工质引自凝结水泵出口时，机组循环热效率随碳捕捉率的增加而提高；当预热段进口工质引自给水泵出口时，机组循环热效率随碳捕捉率的增加而降低，碳捕捉率 100% 时降低 3.47%，明显优于使用汽轮机某级抽汽通过减压降温后作为溶剂再生热源的情况，其所需太阳能集热器场面积远远低于前者。

5 结 论

（1）提出新型抛物槽式太阳能集热系统供能条件下的胺基 CO_2 捕集系统与燃煤机组热力系统的集成工艺，通过扩容蒸发器的合理布置以及回水管路的局部改造，消除了太阳能集热系统两相流区，使得碳捕捉率以及机组热经济性皆得到明显改善。

（2）基于等效焓降法及节能理论，扩容蒸发器中疏水及再沸器回水汇入点为主凝结水管路 6 号加热器出口方案最优。预热段由凝结水泵出口引入水份额为 40% 时，节省标煤耗率 0.31 g/(kW·h)，碳捕捉率达 43.86%，所需太阳能集热器场面积约为 198 525 m^2。

（3）太阳能集热系统预热段进口水引自凝结水泵出口时，机组循环热效率随碳捕捉率的增加而提高；引自给水泵出口时，则与之相反。基于新型太阳能集热系统供能下的胺基 CO_2 捕集系统，在节能减排以及在改善机组热经济性能方面均优于使用汽轮机某级抽汽减压降温后作为溶剂再生热源的传统方式。

参考文献:

[1] 仲伟龙. CO_2 化学吸收技术研究［D］. 杭州：浙江大学，2008.

ZHONG Wei-long. Study of CO_2 chemical absorption technology［D］. Hangzhou：Zhejiang University，2008.

[2] 翟融融. 二氧化碳减排机理及其与火电厂耦合特性研究［D］. 北京：华北电力大学，2010.

ZHAI Rong-rong. Study of the mechanism governing the CO_2 emissions reduction and its coupling characteristics with a thermal power plant [D]. Beijing: North China University of Electric Power, 2010.

[4] 黄　斌，许世森，郜时旺，等. 华能北京热电厂 CO_2 捕集工业试验研究 [J]. 中国电机工程学报，2009，29(17)：14－20.
HUANG Bin, XU Shi-sen, GAO Shi-wang, et al. Industrial experimental study of the CO_2 capture in Huaneng Beijing-based thermal power plant [J]. Proceedings of China Electric Machinery Engineering, 2009, 29(17): 14－20.

[5] 冉　鹏，张树芳，张文宝. 太阳能－地热联合闪蒸发电系统及其㶲评价 [J]. 动力工程学报，2005，25 (sup)：576－579.
RAN Peng, ZHANG Shu-fang, ZHANG Wen-bao. A solar energy-geothermal combined flash power generation systerm and its exergy evaluation [J]. Journal of Power Engineering, 2005, 25 (sup): 576－579.

[6] 高志超，隋　军，刘启斌，等. 抛物槽式太阳能蒸汽发生系统研究 [J]. 工程热物理学报，2011，32 (5)：721－724.
GAO Zhi-chao, SUI Jun, LIU Qi-bin, et al. Study of a parabolic trough type solar energy steam generation system [J]. Journal of Engineering Thermophysics, 2011, 32 (5): 721－724.

[7] CHEN Hai-ping, WANG Jing, LI Ping, et al. Energy consumption analysis of coal-fired power plant with CO_2 capture system based on solar energy [J]. Sustainable Energy, 2011, 11(3): 11－18.

[8] 崔映红，陈　娟，杨　阳，等. 太阳能辅助燃煤热发电系统性能研究 [J]. 中国电机工程学报，2009，29(23)：92－98.
CUI Ying-hong, CHEN Juan, YANG Yang, et al. Study of the performance of a solar energy-aided thermal power generation system [J]. Proceedings of China Electric Machinery Engineering, 2009, 29(23): 92－98.

[9] 林万超. 火电厂系统节能理论 [M]. 西安：西安交通大学出版社，1994：34－59.
LIN Wan-chao. Energy-saving theory for thermal power plants [M]. Xi'an: Xi'an Jiaotong University Press, 1994: 34－59.

（丛　敏　编辑）

新技术、新工艺

DOE 提高效率并降低成本的研究项目

据《Gas Turbine World》2012 年 11－12 月刊报道，U. S. Dept of Energy Advanced Research Projects Agency（美国能源部先进技术研究计划管理局）已授予 Pratt & Whitney Rocketdyne 公司一个总金额超过 500 万美元的合同，用于三个研究项目的费用，以便提高商业规模电站内的燃气轮机效率并降低发电成本。

该计划的第一个研究项目是使用新技术，其是改进天然气生产液体燃料；在与下游的气体到液体过程相结合时，该技术可以用国家的天然气生产汽油，而不是用原油来生产汽油。

ARPA－E（隶属于美国国防部的尖端技术研究计划管理局）声称，该技术有潜力使气体－到－液体转换的成本减少 25%，并也可以用工艺过程中释放的热能发电。

该计划的第二个研究项目是 Rocketdyne 公司将设计并制造连续爆燃的燃烧室，并在模拟燃气轮机环境中进行试验，以便证实该技术用于天然气燃气轮机的可行性。

预期开发用于天然气涡轮技术的连续爆燃发动机燃烧室，将使商业规模电站每年每台燃气轮机的运行费用至少减少 500 万美元。

该计划的第三个研究项目是 Rocketdyne 公司打算开发一种先进的燃气轮机循环；借助于纯氧而不是空气来燃烧燃料，产生非常高的温度，该循环效率可大大提高。

该循环将产生零排放，并有潜力使天然气涡轮的燃料消耗减少 50% 左右，也可以使电厂的效率提高 1 倍，达到 75%，并使电力成本降低 60%。

（吉桂明　摘译）

For a NZK600-16.7/538/538 large-sized coal-fired power generator unit, established was a model for studying the performance of a solar energy auxiliary type thermal system. Based on the thermodynamics first and second law, the authors had analyzed the variation law governing the performance of the unit with load under various alternative versions. It has been found that the heat and power conversion efficiency of the solar energy will increase with an increase of the steam extraction stage number and load. Among them, the second steam extraction section can achieve the highest efficiency, under 100% THA operating condition, the output power of the unit will increase by 6.13% and the coal consumption rate can be saved by 13.14 g/(kW·h). In such a case, the thermal and exergy efficiency will be 39.35% and 39.67% respectively. The economic analytic results show that when the unit is operating in the power increment mode, the investment payback period will be shortened, if the optimum alternative version is adopted, the investment payback period will be around 1.2 years. The research findings can offer theoretical underlying basis and scientific support for designing a solar energy and coal-fired unit mutually complementary power generation system and in the meantime, provide a new thought for optimizing the unit to save more energy. **Key words:** solar energy utilization, solar energy auxiliary feedwater heating, different steam extraction alternative version, exergy analysis, payback period

基于太阳能集热技术的火电厂 CO_2 捕集系统性能研究 = Study of the Performance of a CO_2 Capturing System Based on the Solar Energy Heat Collection Technology **[刊，汉]** CHEN Hai-ping (Research Center for National Thermal Power Generation Project Technology, College of Energy Source, Power and Mechanical Engineering, North China University of Electric Power, Beijing, China, Post Code: 102206), YU Xin-wei, LU Guang-wu (College of Energy Source, Power and Mechanical Engineering, North China University of Electric Power, Baoding, China, Post Code: 071003) //Journal of Engineering for Thermal Energy & Power. -2013, 28(6). -644 ~ 649

In the light of the high energy consumption of the carbon dioxide capturing technology in coal-fired power plants, described was the mechanism governing the coupling among a novel type parabolic trough solar energy heat collection system, amidogen carbon dioxide capturing system and thermal system for a coal-fired power generator unit. Based on the equivalent enthalpy drop method theory, the thermal cost-effectiveness of various integration versions were calculated and analyzed of a 300 MW coal-fired power generator unit. In this connection, the variation law governing the thermal cost-effectiveness of the unit in an amidogen carbon dioxide capturing system and the optimum water returning location and law of the drain water in the flash vaporizer and saturated water from the reboiling vaporizer were obtained. It has been found that when the inlet water of the preheated section is introduced from the outlets of the condensate pumps, the cyclic thermal efficiency of the unit will increase with an increase of the carbon capturing rate. When the inlet water of the preheated section is introduced from the outlets of the feedwater pumps, on the contrary, the optimum water returning location of the saturated water from both flash vaporizer and reboiling one lies in the outlet of the heater No. 6 in the main condensate water pipeline of the unit. When the proportion of the water introduced from the outlets of the condensate pumps in the preheated section was 40%, the standard coal consumption rate saved was 0.31 g/kw. h and the carbon capturing rate attained 43.86%. **Key words:** CO_2 capturing, solar energy heat collection system, equivalent enthalpy drop method, thermal cost-effectiveness

生物质灰结渣判别指数研究 = Study of the Index for Discriminating the Slagging of Ash Produced from Combustion of Biomass **刊,汉** YUAN Rui-bin, LIU Zhi-qiang, XU Ai-qun (College of Energy Science and Engineering, Central China University, Changsha, China, Post Code: 410083), LONG Bing (Changsha Jinzhi Engineering Consultancy Co. Ltd., Changsha, China, Post Code: 410007) //Journal of Engineering for Thermal Energy & Power. -2013, 28(6). -650 ~ 654

By using the coal-produced ash slagging index to discriminate the slagging of ash produced from combustion of biomass, the authors had found that the coal-produced slagging index is incapable of accurately discriminating the slagging of ash produced from combustion of biomass. To study the index for discriminating the slagging of ash produced from combustion of biomass fuel, based on the samples showing the slagging degrees of ash produced from combustion of 40 groups of biomass, a sequence was made from small to big according to their softening temperatures. By using the optimum three-section segmentation method, a model for the limits of softening temperature, alkali/acid ratio, silicon/aluminum ratio and calcium/iron ratio totaling four kinds of commonly seen indexes for discriminating the slagging of ash produced from combustion of biomass was established based on the data specimens. The model in question was used to predict the slagging tendency of ten kinds of biomass. The prediction results show that the use of the model in question can greatly enhance the accuracy in discriminating the slagging tendency of ash produced from combustion of biomass fuels, especially, by employing the calcium/iron ratio, such a slagging tendency can be discriminated with a very high precision. **Key words:** biomass, optimum segmentation, discrimination index, slagging tendency